CARBON 49 (2011) 1075–1086

available at www.sciencedirect.com

ScienceDirect

journal homepage: www.elsevier.com/locate/carbon

Flexible graphite modified by carbon black paste for use as a thermal interface material

Kesong Hu, D.D.L. Chung *

Composite Material Research Laboratory, University at Buffalo, State University of New York, Buffalo, NY 14260-4400, USA

ARTICLE INFO

Article history:
Received 8 September 2010
Accepted 27 October 2010
Available online 26 November 2010

ABSTRACT

Polyol-ester-based carbon black pastes are used to either coat or penetrate flexible graphite, thereby increasing the thermal contact conductance of flexible graphite between copper surfaces. Paste penetration by up to an effective paste thickness (the volume of the penetrated paste divided by the geometric area of the flexible graphite) of 5 μm increases the conductance by up to 350%, 98% and 36% for thicknesses of 50, 130 and 300 μm, respectively. Paste coating up to 10 μm increases the conductance by up to 200%, 120% and 65% for thicknesses of 50, 130 and 300 μm, respectively. The paste penetration is more effective than the paste coating in enhancing the conductance, when the thickness is below 130 μm. At thickness $\geqslant$130 μm, paste penetration and paste coating are similarly effective. These results stem from the relatively low interfacial thermal resistivity provided by paste penetration and the relatively high through-thickness thermal conductivity provided by paste coating. Paste penetration decreases the thermal conductivity of flexible graphite, but paste coating does not affect the conductivity. Both penetration and coating decrease the interfacial resistivity. The highest thermal contact conductance is 1.4×10^5 W/m^2 K, as provided by paste-penetrated flexible graphite of thickness 26 μm.

1. Introduction

Thermal interface materials [1] are needed to improve thermal contacts, which are particularly important for microelectronic cooling. In spite of heat sinks of high thermal conductivity, heat dissipation from the heat source (e.g., a microprocessor) to the heat sink is inadequate unless the thermal contacts in the heat conduction path are sufficiently small in the thermal resistance. Due to the fact that the proximate surfaces of a thermal contact are never perfectly flat or smooth, a thermal interface material must be able to conform to the topography of the proximate surfaces so that the air in the valleys of the surface topography is displaced [2].

There are two main categories of thermal interface materials, namely solids and pastes. Their characteristics are listed in Table S1. Handleability is the main advantage of the solid form. Among the solid materials, flexible graphite is attractive for its resilience and chemical inertness [3]; the thermal-paste-coated metal foils [6] give the highest thermal contact conductance prior to this work; and the silicone-based thermal pads [6] are used most widely. Low minimum thickness and low interfacial resistivity are the main advantages of the paste form, due to the conformability that stems from the fluid nature. Among the thermal interface pastes, the carbon black paste gives high conformability [6] and the silver paste exhibits high thermal conductivity [6].

Flexible graphite is a material that is made by the compression of exfoliated graphite, which is in turn made by the exfoliation of intercalated graphite flake [3]. Due to the accordion-like microstructure of exfoliated graphite, mechanical interlocking between pieces of exfoliated graphite (each piece obtained from a flake being known as a worm) occurs

* *Corresponding author:* Fax: +1 (716) 645 2883.
E-mail address: ddlchung@buffalo.edu (D.D.L. Chung).
URL: http://alum.mit.edu/www/ddlchung (D.D.L. Chung).
0008-6223/$ - see front matter
doi:10.1016/j.carbon.2010.10.058

upon compression. The interlocking enables the formation of a flexible and resilient sheet in the absence of a binder. Due to its resilience in the direction perpendicular to the sheet, flexible graphite is used as a gasket for fluid sealing and as an electromagnetic interference shielding gasket material [5,6]. Related to the resilience is the conformability. Due to its conformability and thermal conductivity, flexible graphite is also used as a thermal interface material [4]. Because of the absence of a binder, flexible graphite is attractive for its chemical resistance and thermal stability.

Thermal interface materials are commonly in the form of a standalone sheet, which facilitates handling. The sheet form of flexible graphite is thus suitable. Although flexible graphite is conformable, it is not as conformable as thermal interface materials in the form of pastes (known as thermal pastes). A particularly conformable type of thermal paste is a paste with carbon black as the solid component and a polyol ester oil as the vehicle. The high conformability of the carbon black paste is due to the conformability of the carbon black solid, which is in the form of porous agglomerates of nanoparticles. This morphology enables carbon black to be "squishable". The squishability is valuable for the conformability and the spreadability. In general, for any thermal interface material, the greater the thickness, the higher is the thermal resistance. Due to its high conformability and spreadability, the carbon black thermal paste [7–10] is much more effective than flexible graphite as a thermal interface material.

By coating both sides of a sheet of commercially made flexible graphite with a carbon black thermal paste, the effectiveness of the flexible graphite as a thermal interface material is significantly enhanced [4]. However, the coated flexible graphite is inferior to aluminum foil that has been similarly coated, due to the large thickness of the flexible graphite compared to aluminum foil [4]. On the other hand, in the absence of the coating, flexible graphite is more effective than aluminum foil [4].

This work is directed at improving the performance of flexible-graphite-based thermal interface materials by allowing a thermal paste to penetrate the flexible graphite. Furthermore, the comparison of the effects of paste coating and paste penetration on the performance, and that of the effects of carbon black pastes with different solid contents and viscosities on the performance of paste-modified flexible graphite, are performed. This work is also directed at studying the effect of the thermal paste on the thermal conductivity and interfacial thermal resistivity of flexible graphite and investigating the effect of the thickness and the fabrication pressure on the performance of flexible-graphite-based thermal interface materials.

2. Experimental methods

2.1. Materials

The exfoliated graphite is obtained by rapid furnace heating of sulfuric acid intercalated graphite, which is known as expandable graphite (made from natural graphite flakes), as provided as expandable flake graphite (Grade 3772) by Asbury Carbons, Asbury, NJ. In this work, the heating is conducted in a stainless steel foil tubing of length 65 cm, with flowing nitrogen, by using a Lindberg tube furnace at 1000 °C, with the expandable graphite flakes exposed to this temperature for 2 min. After exfoliation, the worms (a worm referring to the exfoliated graphite obtained from a single graphite flake) are of length 2–4 mm.

Unless noted otherwise, the carbon black used in making the thermal paste is Vulcan XC72R GP-3820 from Cabot Corp., Billerica, MA. It is a powder with particle size 30 nm, a nitrogen specific surface area 254 m^2/g, maximum ash content 0.2%, volatile content 1.07% and density 1.7–1.9 g/cm^3. The carbon black powder is mixed with a vehicle by hand stirring to form a uniform paste. The paste contains 2.4 vol.% carbon black, which is the optimum volume fraction for high thermal contact conductance [7,9]. An excessive amount of carbon black is detrimental, due to the loss in conformability. A thermal paste containing 1.2 vol.% carbon black of the same type is also studied.

Another type of carbon black used is Tokablack #3800, which is graphitized carbon black supplied by Tokai Carbon Co., Ltd. (Tokyo, Japan). Its particle size is 70 nm, with nitrogen specific surface area 27 m^2/g, maximum ash content 0.02% and volatile content 0.12%. The paste contains 15 vol.% carbon black, which is the volume fraction for providing the highest thermal contact conductance [9]. The technical data for these two kinds of carbon black are shown in Table 1.

The vehicle used for the thermal pastes consists of polyol esters [7], which are attractive for their thixotropic behavior and ability to resist elevated temperatures. The polyol esters in the vehicle are pentaerythritol ester of linear and branched fatty acids and dipentaerythritol ester of linear and branched fatty acids. The polyol ester mixture (Hatcol 2372) is provided by Hatco Corp., Fords, NJ. The specific gravity is 0.97.

Flexible graphite with carbon black paste penetration is prepared by compression of a column of exfoliated graphite in the presence of the paste at the top and bottom surfaces of the exfoliated graphite column. The paste positioned directly above and below the exfoliated graphite column is in the form of a coating on a Teflon sheet. The two coated Teflon

Table 1 – Technical data for the two kinds of carbon black used in this work [9].

Type	DBP[a] (ml/100 g)	Specific surface area (m^2/g)	Particle size (nm)	Agglomerate size (μm)	Maximum volume fraction in random media (%)
Tokablack #3800	60	27	70	20–30	48.1
Cabot XC72R	188	254	30	20–30	23.8

[a] The DBP value is expressed in terms of the volume of dibutyl phthalate absorbed by 100 g of carbon black. A greater amount of absorption indicates a higher structure.

sheets (50 μm thick) are oriented perpendicular to the axis of the column. The compression is conducted in a cylindrical mold of length 45 cm and inner diameter 31.7 mm by applying a uniaxial pressure via a matching piston. The pressure is 11.2 MPa (2000 lb), unless stated otherwise. Other pressures used are 5.6 MPa (1000 lb), 16.8 MPa (3000 lb) and 28.0 MPa (5000 lb). The pressure is held for 10 min. A part of the paste penetrates the flexible graphite as the flexible graphite is formed. The penetrant coats the surfaces of the worms, rather than filling the voids in the flexible graphite sheet. The entire thickness of a flexible-graphite-based specimen is obtained in one 11.2 MPa compression stroke. Each resulting specimen is a disc of diameter 31.7 mm. The thickness varies slightly among the specimens, as controlled by the amount of exfoliated graphite in the column, and is separately measured for each specimen. Specimens of the corresponding unmodified flexible graphite are similarly prepared, except that a paste is not used.

In the case of paste-coated flexible graphite, one layer of thermal paste is applied by brushing (like painting) directly on each side of an unmodified flexible graphite specimen made beforehand at a pressure of 11.2 MPa (2000 lb) with the absence of a paste in the column. The thickness of the coating is controlled by controlling manually the brushing force.

The minimum thickness of the flexible graphite is limited by the fragility of the specimens, which may fracture during the separation from the Teflon sheets after compression. The minimum thickness of unmodified flexible graphite is about 30 μm. With each coating being about 10 μm thick and the presence of a coating on either side, the minimum thickness of paste-coated flexible graphite is about 50 μm. When the 15 vol.% Tokai paste is used as a penetrant, the minimum thickness is 42 μm. When the 2.4 vol.% Cabot paste is used as a penetrant, the minimum thickness is 26 μm. That the minimum thickness is larger for the Tokai paste is due to its higher degree of stickiness.

2.2. Thermal contact conductance measurement

The guarded hot plate method (ASTM Method D5470) [4,7] is a well-established steady-state method for the measurement of the thermal contact conductance of thermal contacts. In this method, a thermal interface material is sandwiched between two copper cylinders which are 1.25 in (31.7 mm) in diameter. The surface of the two proximate surfaces of the copper cylinders has been polished by 600 grit sandpaper and the roughness is 15 μm, which is the roughness used in prior work [4,7] and referred to as the rough case. The height of each copper cylinder is 35 mm. Each cylinder has centered holes located at a distance of 5 mm from each end of the cylinder. Each hole is for the insertion of a type-T thermocouple.

The heating element is a metal coil embedded in a copper block (76 mm × 76 mm) to serve as the heat source. The heating power is controlled by a temperature controller. The top copper cylinder in contact with and below the heat source is thermally insulated at its sides by using glass fiber cloth in order to minimize lateral heat loss. Below the bottom copper cylinder is a water-cooled copper heat sink (76 mm × 76 mm).

The temperature gradient is determined from the temperature difference of the two holes in each copper cylinder, which is $T_1 - T_2$ and $T_3 - T_4$, respectively. The equality of these two differences indicates the attainment of equilibrium, in principle. However, in this work, the average value of these two quantities, divided by 25 mm, is taken as the temperature gradient when these two quantities differ by less than 0.5 °C. The heating was maintained for 30 min after the heating element has reached 100 °C in order to reach equilibrium. A commercial thermal grease is used to coat each thermocouple probe, which is held in each hole for 10 min for each temperature measurement. The pressure applied on the interface is provided by a screw load cell and monitored by a strain gauge. A pressure of 0.46 MPa is used in this work. The experimental set-up is as illustrated in Fig. S1.

The heat flow Q is a function of the temperature gradient $(\Delta T/d_A)$, i.e.

$$Q = \frac{\lambda A}{d_A}\Delta T \tag{1}$$

where λ is the thermal conductivity of the copper block, A is the area of the copper cylinder, and d_A is the distance of 25 mm between two temperature recording holes within one copper cylinder.

The temperatures of both the top and bottom of the thermal interface material, T_A and T_D, are given by

$$T_A = T_2 - \frac{d_B}{d_A}(T_1 - T_2) \tag{2}$$

and

$$T_D = T_3 + \frac{d_D}{d_C}(T_3 - T_4) \tag{3}$$

where d_B is the distance between temperature recording hole T_2 and the bottom surface of the upper copper cylinder (5 mm), d_C is the distance between two temperature recording holes within one copper cylinder (25 mm), and d_D is the distance between temperature recording hole T_3 and the top surface of the lower copper cylinder (5 mm). Since the geometry dimensions of the two copper cylinders are the same, the Eqs. (2) and (3) can be simplified to

$$T_A = T_2 - \gamma\Delta T \tag{4}$$

and

$$T_D = T_3 + \gamma\Delta T \tag{5}$$

where γ is a geometric parameter (i.e. 5 mm/25 mm = 0.2).

The thermal resistivity θ is given by

$$\theta = (T_A - T_D)\frac{A}{Q} \tag{6}$$

Insertion of Eqs. (1), (4), and (5) into Eq. (6) gives θ, which is independent of the area A, i.e.

$$\theta = \left(\frac{T_2 - T_3}{\Delta T} - 2\gamma\right)\frac{d_A}{\lambda} \tag{7}$$

The reciprocal of θ is the thermal contact conductance.

2.3. Thermal conductivity and interfacial thermal resistance measurement

The through-thickness thermal conductivity of a thermal interface material is calculated from the thermal contact

conductance (Section 2.2), as explained below. The total thermal resistance R between the heat source and the heat sink is

$$R = \frac{h}{kA} + R_1 + R_2 \quad (8)$$

where h is the thickness of the interface material, k is the thermal conductivity of the interface material, and R_1 and R_2 (equal in this case and denoted as R_i) are the interfacial thermal resistance of the interface between the interface material and the two copper cylinders. The total thermal resistance R is the inverse of the thermal contact conductance (C) divided by area A. Thus, Eq. (8) becomes

$$\frac{1}{C} = \frac{h}{k} + 2R_iA \quad (9)$$

For a specific thermal interface material, the thermal conductivity of the material and the interfacial resistance R_i can be determined by testing a series of specimens of various thicknesses and linear fitting of the data pairs of 1/C and h. The inverse of the slope of the fitted line is the thermal conductivity and the intercept at the vertical axis divided by 2A is the interfacial resistance R_i. At least three specimens of each type were tested.

2.4. Thickness measurement

The thickness of a thermal interface material greatly affects its effectiveness. As shown by (9), with all other parameter fixed, the larger the thickness h, the lower is the thermal contact conductance C. The thickness of a specimen is measured at five points by using a micrometer. The thickness deviation within a specimen is 3–9 μm and diminishes with decreasing thickness.

The thickness of a paste coating was measured by several methods in prior work [9,11]. The so-called direct method [9] uses a strain gauge fixed on a steel spring to measure the microscale vertical displacement of the two proximate copper surfaces. However, the accuracy is inadequate when the coating thickness is small. Another method, called the indirect method [11], determines the thickness of the coating by measuring the diameter of the coating area with controlled volume.

In this work, a new method is introduced to determine the thickness of the paste coating. It is also an indirect method. However, instead of measuring the diameter of the coated area, the weight of the paste used to coat is measured. Since the flexible graphite surface is fully covered by the paste and the density of the paste is known, the weight of the paste is used to calculate the thickness of the paste. This method is as accurate as the direct method because of the high sensitivity of the weighing (0.01 mg).

In relation to the pasted-penetrated specimens, the method of measurement of the penetrated thermal paste volume involves separately weighing the worms prior to compression and the composite after compression. The weight of the penetrated paste is then given by the difference between these two quantities. The effective thickness of the penetrated paste is taken as the volume of the penetrated paste divided by the area of the thermal interface material.

2.5. Viscosity measurement

The effectiveness of a thermal paste as a coating or a penetrant is sensitive to its viscosity. The viscometer used in this work is the LVT Dial-Reading Viscometer from Brookfield Engineering Laboratories, Inc., Middleboro, MA, with Model SSA-18/13R Small Sample Adaptor.

2.6. Microstructural examination

The microstructure of the exfoliated graphite, the carbon black particles and the paste coated/penetrated flexible graphite was observed by an optical microscope and a scanning electron microscope (SEM) in the secondary electron imaging mode.

3. Results and discussion

3.1. Density

The density of unmodified flexible graphite is 1.21 ± 0.04 g/cm^3, which is lower than the value of 2.27 g/cm^3 for ideal graphite [12], indicating that the porosity of the unmodified flexible graphite is 44%. The density of unmodified flexible graphite is higher than the value of 0.08 g/cm^3 reported by Wei et al. [13] for flexible graphite compressed at the same pressure, due to the confined compression used in this work, in contrast to the rolling compression used by Wei et al.

3.2. Thermal conductivity, interfacial resistance and paste thickness

Table 2 shows the through-thickness thermal conductivity, interfacial resistance and the thermal paste thickness of the modified flexible graphite. The thermal conductivity is obtained from the slope of the curve in Fig. 1, whereas the interfacial resistivity is obtained from the intercept of the curve with the vertical axis of Fig. 1. In spite of the low density of 1.21 g/cm^3 compared to the value of 2.27 g/cm^3 [12] for highly oriented pyrolytic graphite (HOPG), the through-thickness thermal conductivity of the unmodified flexible graphite is 5.8 W/m K, which is higher than the value of 4.8 W/m K for HOPG [14] at the temperature of 350 K. This is because of the microstructural network in the flexible graphite, in contrast to the highly oriented layer structure of HOPG. The through-thickness thermal conductivity is close to the value of 6.0 W/m K reported by Wei et al. [13] for flexible graphite at the same density.

The through-thickness thermal conductivity is not affected by the paste coating. The thermal conductivity values of the flexible graphite coated by the two types of paste (Cabot and Tokai) are similar, namely 5.9 W/m K. This means that the coating does not affect the microstructure of the heat conduction network. The thermal conductivity of the 2.4 vol.% Cabot paste is 0.128 ± 0.001 W/m K, and that of the 15 vol.% Tokai paste is 0.331 ± 0.002 W/m K [11] – both much lower than that of the unmodified flexible graphite. The paste coating is very thin (7.6 μm for the 2.4 vol.% Cabot coating and 10.5 μm for the 15 vol.% Tokai coating) compared to the

Table 2 – Thermal conductivities, interfacial resistances and coating thicknesses of paste-modified flexible graphite specimens. Real paste thickness applies to the specimens with paste coatings. Effective paste thickness applies to the specimens with paste penetration.

Composition	Fabrication pressure		Linear fit of the dependence of the thermal resistivity (y) on the thickness (x) (Fig. 1)	Thermal conductivity (W/m K)	Interfacial resistivity (10^{-6} m^2 K/W)	Real/effective paste thickness	
	lb	MPa				μm	% of composite thickness
Unmodified	2000	11.2	$y = 0.1721x + 5.4 \times 10^{-5}$, $R^2 = 0.9955$	5.8 ± 0.8	54.2 ± 2.2	0	0
2.4 vol.% Cabot coated	2000	11.2	$y = 0.1707x + 1.2 \times 10^{-5}$, $R^2 = 0.9935$	5.9 ± 0.5	12.4 ± 1.0	7.6 ± 1.2	22.7
15 vol.% Tokai coated	2000	11.2	$y = 0.1705x + 1.3 \times 10^{-5}$, $R^2 = 0.9892$	5.9 ± 0.9	12.9 ± 3.0	10.5 ± 2.2	26.5
1.2 vol.% Cabot penetrated	3000	16.8	$y = 0.2871x + 1.3 \times 10^{-6}$, $R^2 = 0.9983$	3.5 ± 0.1	1.35 ± 0.84	6.7 ± 0.3	16.5
2.4 vol.% Cabot penetrated	3000	16.8	$y = 0.2639x + 1.3 \times 10^{-6}$, $R^2 = 0.993$	3.8 ± 0.3	1.35 ± 0.68	5.1 ± 1.9	12.6
15 vol.% Tokai penetrated	3000	16.8	$y = 0.2537x + 1.3 \times 10^{-6}$, $R^2 = 0.9969$	3.9 ± 0.5	1.30 ± 0.11	3.7 ± 1.5	9.1

thickness of the unmodified flexible graphite substrate (50–250 μm), so its contribution to the thermal conductivity of the composite is negligible.

The through-thickness thermal conductivity is decreased by the paste penetration by 33–40%. This is because the pressure used in making the penetrated specimens causes the paste to penetrate the forming flexible graphite, thereby partially interrupting the interlocking network. In contrast, the coating method is effective for maintaining the thermal conductivity of the flexible graphite.

The thermal conductivity of the flexible graphite penetrated with the 1.2 vol.% Cabot paste is slightly lower than the flexible graphite penetrated with the 2.4 vol.% Cabot paste or the 15 vol.% Tokai paste. This is due to the low carbon black content in the 1.2 vol.% Cabot paste. The conductivity is low for the flexible graphite penetrated with the 1.2 vol.% Cabot paste, in spite of the high effective paste thickness (Table 2). This is due to the low viscosity of the 1.2 vol.% Cabot paste (Section 3.5). Excessive fluidity of the paste causes more disruption to the conduction network of the flexible graphite, thereby decreasing the thermal conductivity.

The interfacial thermal resistivity of the unmodified flexible graphite interfacing with copper is $5.4 \times 10^{-5+}$m^2 K/W. Due to the through-thickness resilience (hence, high conformability) of flexible graphite, the interfacial resistivity of flexible graphite is lower than that of metal foils (7.9×10^{-5} m^2 K/W for aluminum and 1.3×10^{-4} m^2 K/W for copper) [4]. Nevertheless, the interfacial resistance contributes significantly to the thermal resistance of the overall thermal contact. The interfacial resistivity of the paste-coated flexible graphite is 1.3×10^{-5} m^2 K/W, which is lower than that of the unmodified flexible graphite (5.4×10^{-5} m^2 K/W). The interfacial resistivity of the paste-penetrated flexible graphite is 1.4×10^{-6} m^2 K/W, which is lower than that of the paste-coated flexible graphite by an order of magnitude.

The reason for the low interfacial resistivity of the paste-coated flexible graphite compared to the unmodified flexible graphite is that the high conformability of the paste coating provides better contact with the copper cylinders. The even lower interfacial resistivity of the paste-penetrated flexible graphite is because the paste wets the surface of the worms to form a boggy layer, which in turn increases the conformability of the flexible graphite itself. A higher conformability of the flexible graphite itself helps reduce the air gap at the interface with each copper cylinder. In addition, the absence of a paste layer on the exterior surface of the penetrated flexible graphite is advantageous, due to the low thermal conductivity of the paste compared to flexible graphite (Section 3.2).

As shown in Table 2, the paste thickness is 7–11 μm for the coated flexible graphite and is effectively 4–5 μm for the corresponding penetrated flexible graphite. The effective paste thickness for the paste-penetrated flexible graphite describes the amount of the penetrated paste, as calculated by dividing the volume of the penetrated paste by the geometric area of the flexible graphite. The 15 vol.% Tokai coating is thicker than the 2.4 vol.% Cabot coating. The effective penetrant thickness is smaller for the 15 vol.% Tokai penetrant than the 2.4 vol.% Cabot penetrant. All their

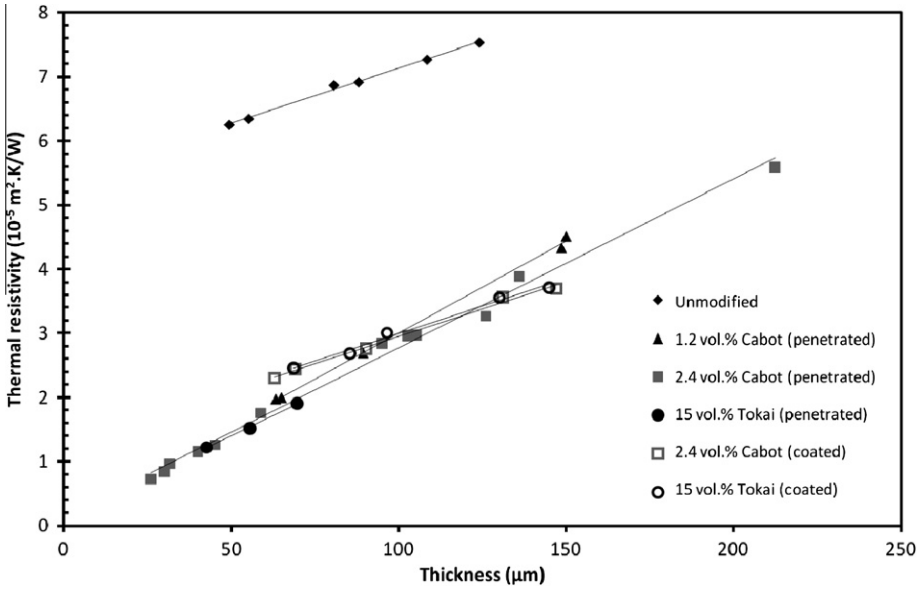

Fig. 1 – Dependence of the thermal resistivity of the thermal contact on the thickness of the different types of flexible graphite.

thicknesses are less than 27% of the thickness of the composite.

The variation of the real/effective paste thickness of different flexible graphite modifications is explained by the difference in viscosity of the pastes. The real thickness of the paste on the coated flexible graphite is higher than the effective paste thickness of the corresponding penetrated flexible graphite, because the 16.8 MPa (3000 lb) pressure during the production of the penetrated specimens caused a part of the paste to be squeezed out. In contrast, the coating method involved no squeezing out of the paste.

The real thickness of the coating of the 15 vol.% Tokai coated specimen is higher than that of the 2.4 vol.% Cabot coated specimen. The viscosity of 15 vol.% Tokai thermal paste is higher than that of the 2.4 vol.% Cabot thermal paste [11], so more paste is left in the flexible graphite surface after the compression for the former. For the same viscosity reason, the effective paste thickness in the penetrated flexible graphite is lower for the former. In other words, due to the higher viscosity, less of the 15 vol.% Tokai paste penetrates the flexible graphite and hence more of it is squeezed out, compared to the 2.4 vol.% Cabot paste. This explains the difference in the effective paste thickness of the 15 vol.% Tokai penetrated flexible graphite and the 2.4 vol.% Cabot penetrated flexible graphite.

3.3. *Thermal contact conductance*

Table 3 shows the values of the thermal contact conductance for various thermal interface materials at three specific thicknesses. Fig. 2 shows the variation of the thermal contact conductance with the thickness. The data points in Fig. 2 fit the model curve well. When the thickness is below 130 μm, the thermal contact conductance of the paste-penetrated flexible graphite is higher than that of the paste-coated or unmodified flexible graphite (Fig. 2). The highest conductance achieved is 13.8×10^4 W/m^2 K for 2.4 vol.% Cabot paste-penetrated flexible graphite at the thickness of 26 μm. Unmodified flexible graphite gives the lowest conductance at the same thickness. This difference in conductance at the same thickness increases as the thickness diminishes. The conductance is governed by the thermal conductivity, thickness and interfacial resistance, as explained in Sections 2.2 and 2.3. At small thicknesses, the interfacial resistance mainly governs the

Table 3 – Thermal contact conductance of selected paste-modified flexible graphite specimens.

Composition	Thermal contact conductance (10^4 W/m^2 K)		
	Thickness[a]		
	50 μm	130 μm	300 μm
Plain	1.59 ± 0.01	1.31 ± 0.01	0.95 ± 0.01
2.4 vol.% Cabot coated	4.78 ± 0.07	2.90 ± 0.03	1.57 ± 0.01
15 vol.% Tokai coated	4.67 ± 0.07	2.86 ± 0.03	1.56 ± 0.01
2.4 vol.% Cabot penetrated	6.90 ± 0.21	2.82 ± 0.05	1.24 ± 0.01
15 vol.% Tokai penetrated	7.17 ± 0.23	2.93 ± 0.04	1.29 ± 0.01

[a] Based on the model curves in Fig. 2.

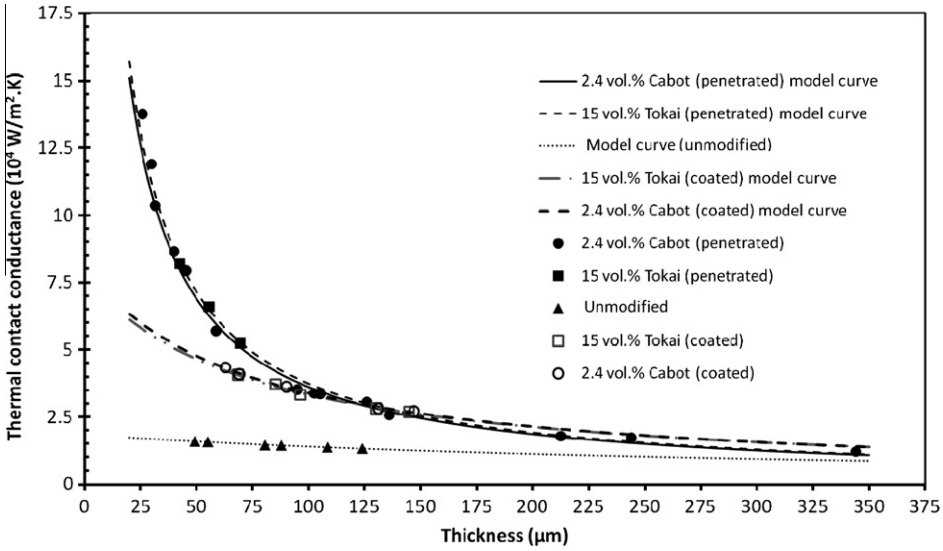

Fig. 2 – Thermal contact conductance and model curves of the selected types of paste-modified flexible graphite.

conductance. Thus, the paste-penetrated flexible graphite is superior to the paste-coated flexible graphite, which is in turn superior to the unmodified flexible graphite. When the thickness exceeds 130 μm, the paste-coated flexible graphite performs essentially equally as the paste-penetrated flexible graphite in terms of the conductance and the unmodified flexible graphite is slightly inferior to the paste-modified flexible graphite. The difference in conductance at the same thickness diminishes as the thickness increases. The impact of the thermal conductivity increases with increasing thickness. Since the thermal conductivity is similar for the various compositions (Table 2), the difference in conductance becomes smaller as the thickness increases.

3.4. *Microstructure*

As shown in Fig. 3, the surface topography of unmodified flexible graphite is fairly smooth, in spite of some random nicks. The topography of the Cabot/Tokai paste-penetrated flexible graphite is rougher; clustered surface pores are present. Fig. 3(d) shows that the topography of the 2.4 vol.% Cabot paste-coated flexible graphite is even smoother than that of the unmodified flexible graphite (Fig. 3(a)), due to the presence of the paste coating. The individual carbon black particles cannot be observed in the coating. Fig. 3(e) shows the topography of the 15 vol.% Tokai paste-coated flexible graphite. The Tokai carbon black forms a cracked crust on the surface of the specimen. Both Fig. 3(d) and (e) show aligned striations that are imprinted by the copper cylinders, thus indicating that the paste-coated flexible graphite is more conformable than the unmodified flexible graphite, which does not show striations. The striations are particularly clear in Fig. 3(e), due to the large thickness of the coating. The higher conformability is also reflected by the lower interfacial resistance compared to the unmodified flexible graphite (Table 2). Fig. 3(f) shows the particle morphology of the Tokai carbon black coating. The particles remain spherical and are loosely connected with each other.

Fig. 4 shows the edge fracture surface (surface perpendicular to the plane of the flexible graphite sheet), as obtained by flexure. Layers that are preferentially oriented in the plane of the flexible graphite were observed for the unmodified, paste-penetrated and paste-coated flexible graphite. Each layer is a stack of graphite atomic layers. For the unmodified flexible graphite (Fig. 4(a)), the graphite layers are crooked and wrinkles occur on the surface of the layers. There is also a feather-like feature at the extremities of some of the layers, due to the tapering of the layers.

The 2.4 vol.% Cabot paste-modified specimens (penetrated or coated), as shown in Fig. 4(b) and (c), are both similar in the fracture morphology to unmodified flexible graphite. On the other hand, the fracture morphology differs between flexible graphite that has been penetrated with the 15 vol.% Tokai thermal paste and flexible graphite that has been coated with the same paste, as shown in Fig. 4(d) and (e). The graphite layers do not show wrinkles for the former, but show wrinkles for the latter. This is because the thermal paste in the former covers the surface of the layers, thereby making the wrinkles not observable. The absence of wrinkles occurs throughout the thickness of the flexible graphite, implying that the penetration is throughout the thickness.

For the paste-coated specimens, no matter Cabot or Tokai (Fig. 4(c) and (e)), the fracture morphology is essentially the same as that of the unmodified flexible graphite. The layers are crooked, with wrinkles. Since no paste penetrated the pre-compressed flexible graphite in the coated case, the microstructure of the thermal-paste-coated specimens remains the same as that of unmodified flexible graphite. This unmodified microstructure is consistent with the experimental result that the thermal conductivity of the paste-coated flexible graphite is as high as that of the unmodified flexible graphite.

The difference of fracture morphology between the Cabot and Tokai paste-penetrated specimens is mainly caused by the difference in the carbon black volume fraction. The high carbon black content in the 15 vol.% Tokai paste causes the paste to cover the graphite layers after penetration. Although

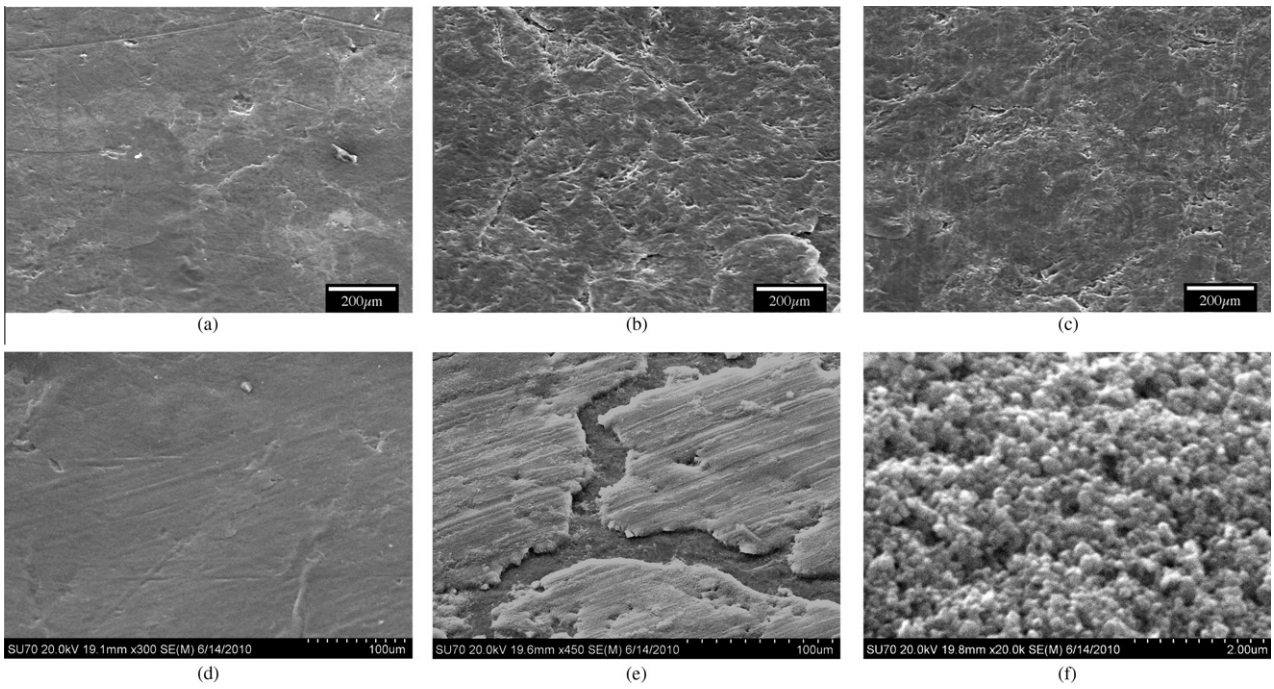

Fig. 3 – SEM photographs. Topography of the surface in the plane of the thermal contact. (a) Unmodified flexible graphite. (b) 2.4 vol.% Cabot paste-penetrated flexible graphite. (c) 15 vol.% Tokai paste-penetrated flexible graphite. (d) 2.4 vol.% Cabot paste-coated flexible graphite. (e) 15 vol.% Tokai paste-coated flexible graphite. (f) Tokai carbon black particles in the coating.

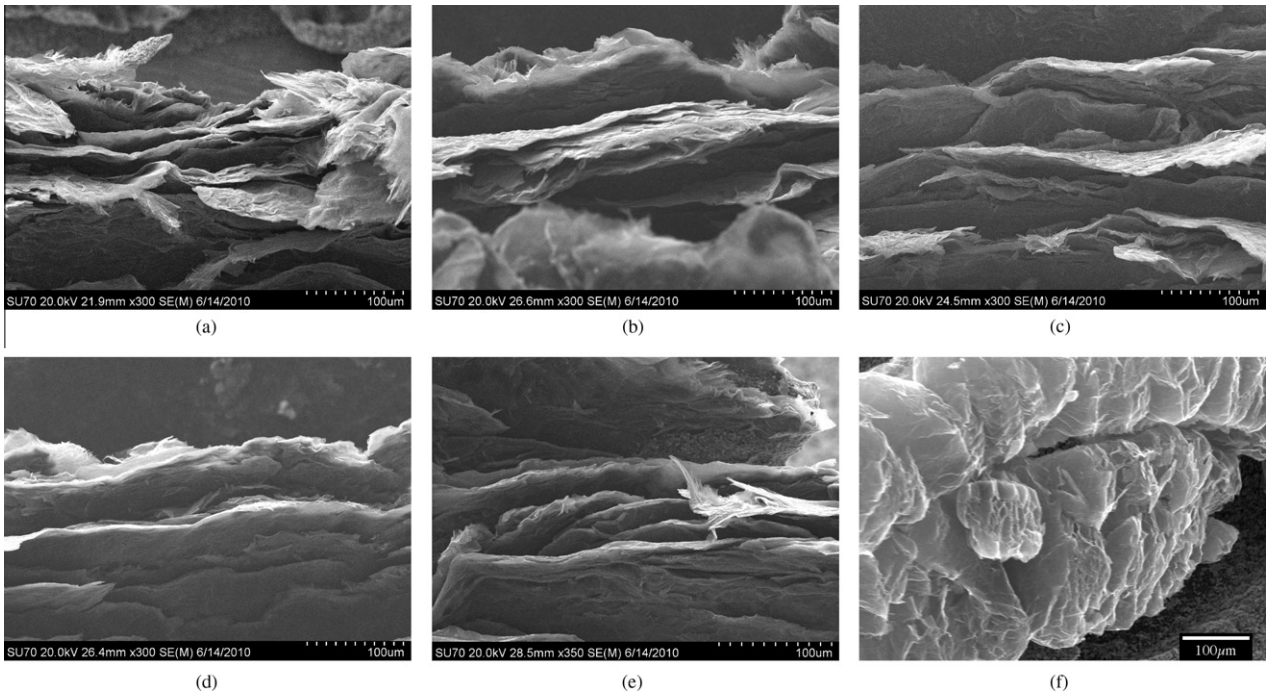

Fig. 4 – SEM photographs. Edge fracture surface obtained by flexure. (a) Unmodified flexible graphite. (b) 2.4 vol.% Cabot paste-penetrated flexible graphite. (c) 2.4 vol.% Cabot paste-coated flexible graphite. (d) 15 vol.% Tokai paste-penetrated flexible graphite. (e) 15 vol.% Tokai paste-coated flexible graphite. (f) Morphology of exfoliated graphite.

such covering is not observed in case of the 2.4 vol.% Cabot thermal paste, due to the low carbon black content, the paste has indeed penetrated the flexible graphite, as indicated by the similarity in thermal conductivity between the Tokai paste-penetrated and Cabot paste-penetrated materials (Table 2).

Fig. 4(f) shows the morphology of exfoliated graphite. The accordion microstructure [11,15], which is typical of exfoliated graphite, is observed. The density and volume of the pores also support the occurrence of exfoliation [16].

The morphology of the peeled surface (as obtained by manual peeling of a surface layer) is also observed, as shown in Fig. 5. Fig. 5(d–f) are higher magnification images corresponding to Fig. 5(a–c), respectively. The graphite sheets are relatively large for the unmodified flexible graphite, are smaller for the Cabot paste-penetrated flexible graphite and even smaller for the Tokai paste-penetrated flexible graphite.

3.5. Viscosity

When a paste is used as a penetrant, a lower viscosity is expected to give a higher degree of penetration and more uniform distribution. When the paste is used as coating, a lower viscosity is expected to give higher conformability of the paste-coated surface [9].

The viscosities of the pastes decrease with increasing shear rate, as shown in Fig. S2, as expected for shear thinning. The result of 2.4 vol.% Cabot paste is similar to prior work [9]. The small difference between these two results is due to that the small volume of paste tested in this work limiting the choice of spindles. At the same shear rate, the viscosity of pristine polyol ester is the lowest; the viscosity of the 1.2 vol.% Cabot thermal paste is a little higher than that of the polyol ester; and the viscosity of 2.4 vol.% Cabot thermal paste is the highest. This difference in viscosity increases when the shear rate decreases. These results indicate that the presence of carbon black increases the viscosity of a paste. The particles interact with the polyol ester molecules, thus impeding the shear movement of the paste. As the shear rate increases, the particles and molecules start to align to a degree, thereby decreasing the shear resistance.

3.6. Effect of the fabrication pressure

Wei et al. [13] showed that the fabrication pressure strongly affects the through-thickness thermal conductivity of the unmodified flexible graphite. However, as shown for the 2.4 vol.% Cabot paste-penetrated flexible graphite in Fig. 6, various fabrication pressures from 1000 lb (5.6 MPa) to 5000 lb (28.0 MPa) give data points that fall on the model curve for the 2000 lb (11.2 MPa) pressure. At the same thickness of 215 μm, the fabrication pressure of 2000 lb (11.2 MPa) and 3000 lb (16.8 MPa) gave essentially the same value of the thermal contact conductance, as shown in Fig. 6. This means that the fabrication pressure affects the conductance through its effect on the thickness and its effect on the microstructure does not affect the conductance. The mechanical integrity of the specimens becomes unacceptable when the pressure is below 2000 lb.

3.7. Comparison with prior work

The paste penetration of flexible graphite increases the thermal contact conductance, thereby enabling the modified flexible graphite to be comparable to or better than any of the previously reported thermal interface materials, which include thermal pastes [4,7,11], paste-coated metal foils [4], silicone-based thermal pads [4,17,18], carbon nanotube arrays [19,20] and silver nanofiber arrays [21]. Table 4 shows the

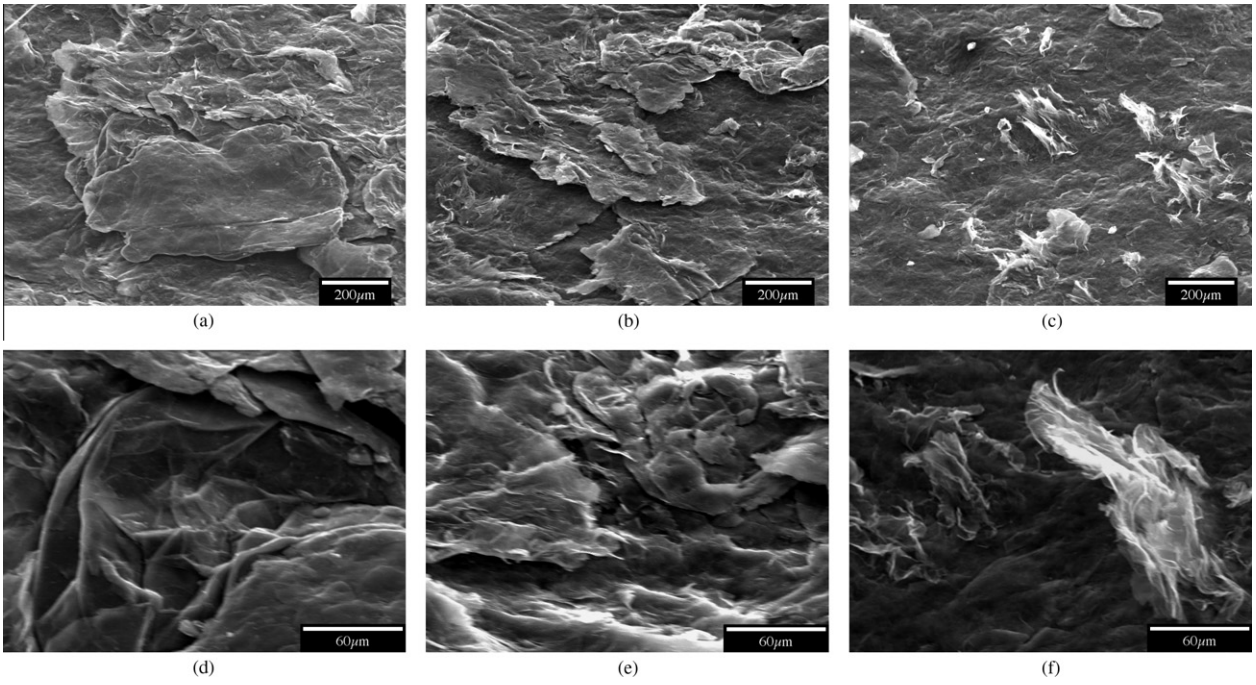

Fig. 5 – SEM photographs. In-plane morphology after manual peeling of the surface. (a) Unmodified flexible graphite. (b) 2.4 vol.% Cabot paste-penetrated flexible graphite. (c) 15 vol.% Tokai paste-penetrated flexible graphite. (d), (e) and (f) are higher magnification views of (a), (b) and (c), respectively.

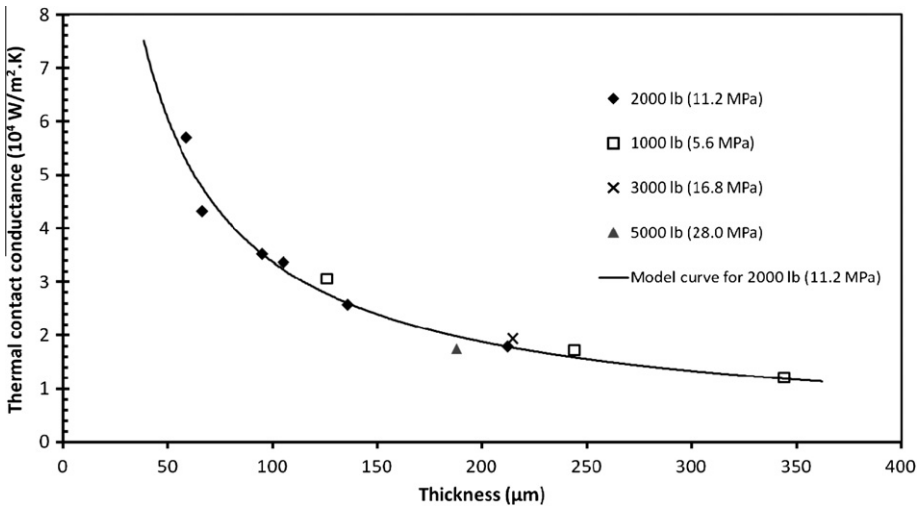

Fig. 6 – Dependence of the thermal contact conductance on the thickness for 2.4 vol.% Cabot paste-penetrated flexible graphite fabricated at various pressures.

comparison among these thermal interface materials in terms of their thermal properties.

Flexible-graphite-based thermal interface materials are advantageous over thermal pastes in their handleability, lower tendency for seepage and larger thickness. The handleability relates to its solid form. A large thickness cannot be provided by a paste without a high tendency for seepage, but it is needed in practice for gap filling.

The minimum thickness of flexible-graphite-based materials (30 μm) tends to be larger than that of metal-foil-based materials (7 μm [4]). This gives the metal-foil-based material an advantage. However, metal foils cannot be modified by paste penetration.

The minimum thickness of silicone-based pads is 200 μm [4], which is much larger than that of flexible-graphite-based materials (30 μm). The large thickness causes the silicone-based pads to exhibit very low values of the thermal contact conductance [4].

The minimum thickness of a carbon nanotube array is 30–207 μm [19,20], which is close to the value of 30 μm for a flexible-graphite-based material. Although the array exhibits high thermal conductivity (19.8 W/m K), the interfacial thermal resistivity is high (1.4×10^{-4} m^2 K/W), thereby resulting a relatively low value of the thermal contact conductance (3×10^3 W/m^2 K [19]) compared to the best paste-penetrated flexible graphite (1.4×10^5 W/m^2 K).

Thermal interface materials in the form of phase change materials (such as those based on wax [22]) are attractive for their being in the solid state at room temperature, so that no seepage can occur during system transportation at room temperature. During operation, due to the temperature rise, the phase change material melts and seepage may occur. In

Table 4 – Comparison of thermal interface materials in terms of the minimum thickness, thermal conductivity, interfacial thermal resistivity and thermal contact conductance.

Material	Minimum thickness (μm)	Thermal conductivity (W/m K)	Interfacial resistivity (10^{-6} m^2 K/W)	Thermal contact conductance (10^4 W/m^2 K)
Paste-penetrated flexible graphite (this work)	26	3.8	1.3	14
Thermal paste [4,7,11]	0.4[a]	0.3	13	12
Aluminum foil [4]	7	237	79	1.3
Thermal-paste-coated aluminum foil [4]	50	237	13	3.7
Carbon nanotube array [19,20]	30–207	3–20	140	0.3
Silver nanofiber array [21]	2000	30	350	2.0
Silicone-based thermal pad [4,17,18]	200	6	N/A	1.0

[a] Contact pressure = 0.46 MPa.

contrast, seepage cannot occur from paste-penetrated flexible graphite at room or elevated temperatures.

The thermal contact conductance of the unmodified flexible graphite at a thickness of 130 μm is $(1.31 \pm 0.01) \times 10^4$ W/m^2 K, which is consistent with the prior report of $(1.40 \pm 0.09) \times 10^4$ W/m^2 K by Leong et al. [4]. The difference is due to the difference in fabrication conditions, as Leong et al. used commercially available flexible graphite made at an undisclosed pressure.

The thermal contact conductance of the 2.4 vol.% Cabot paste-coated flexible graphite at a thickness of 130 μm is $(2.90 \pm 0.03) \times 10^4$ W/m^2 K, which is higher than the value of $(2.34 \pm 0.16) \times 10^4$ W/m^2 K for commercial flexible graphite coated with the same paste and the value of $(1.74 \pm 0.15) \times 10^4$ W/m^2 K for silver-paste-coated flexible graphite [4]. This difference is probably due to the larger coating thickness of Leong et al. inferior conformability of the silver paste and the difference in flexible graphite fabrication condition.

The highest thermal contact conductance attained in this work is 1.4×10^5 W/m^2 K, as provided by a 26-μm thick paste-penetrated flexible graphite. This value is higher than those of carbon nanotube arrays (3×10^3 W/m^2 K) [19], silver nanofiber arrays (2×10^4 W/m^2 K) [21], paste-coated metal foils (3.7×10^4 W/m^2 K) [4] and thermal greases (2×10^4–4×10^4 W/m^2 K) [23]. This value is also higher than any of the previously reported thermal interface materials that involve a thermal paste, as measured under the same condition (15 μm roughness, and 0.46 MPa pressure between copper surfaces). For example, the thermal contact conductance of the 2.4 vol.% Cabot carbon black paste is 8.7×10^4 W/m^2 K [7,11]; that of the 15 vol.% Tokai carbon black paste or the 2.4 vol.% graphite nanoplatelet paste is 1.2×10^5 W/m^2 K [11]. The thickness of either of these two pastes is less than 1.4 μm. Such a small thickness limits the applicability, due to the typically imperfect flatness and parallelism of the proximate surfaces. The thickness range in this work (26 μm or above) is more practical.

In case of smooth (0.009–0.05 μm) copper surfaces, the highest thermal contact conductance reported is 4.0×10^5 W/m^2 K, as obtained for a nanoclay paste [24]. The carbon black paste is less effective than the nanoclay paste in case of smooth surfaces, giving thermal contact conductance up to $(3.0 \pm 0.1) \times 10^5$ W/m^2 K [7,10]. Boron nitride particle filled wax above the melting temperature of the wax (a phase change material) is even less effective, also in case of smooth surfaces, giving thermal contact conductance 1.8×10^5 W/m^2 K [22]. Boron nitride particle filled silicone is still even less effective, also in case of smooth surfaces, giving thermal contact conductance 1.1×10^5 W/m^2 K [25]. As previously reported, the conductance is higher for smoother surfaces for the same thermal interface material [7,10,24]. This work only addresses the case of rough surfaces.

The interfacial resistivity of the Cabot paste-coated flexible graphite is $(1.2 \pm 0.1) \times 10^{-5}$ m^2 K/W, which is consistent with the value of $(1.1 \pm 0.6) \times 10^{-5}$ m^2 K/W for the 2.4 vol.% Cabot paste [11]. The interfacial resistivity of the Tokai paste-coated flexible graphite is $(1.3 \pm 0.3) \times 10^{-5}$ m^2 K/W, which is close to the value of $(7.2 \pm 1.3) \times 10^{-6}$ m^2 K/W for the 15 vol.% Tokai paste [11]. The lowest interfacial resistivity in this work is $(1.3 \pm 0.1) \times 10^{-6}$ m^2 K/W, as provided by the paste-penetrated flexible graphite; this value is lower than those of pastes [11] or paste-coated flexible graphite by an order of magnitude. The low interfacial resistivity of the paste-penetrated flexible graphite compared to the paste-coated flexible graphite is due to the greater conformability of the former. The low interfacial resistivity of the paste-penetrated flexible graphite compared to the paste is due to the solid nature of the paste-penetrated flexible graphite promoting phonon related heat transfer across the part of the interface at which the interface material and copper make direct contact.

The thermal conductivity of flexible graphite with or without paste introduction is low compared to that of metal foils (401 W/m K for copper [14]), silver nanofiber array (30.3 W/m K [21]), carbon nanotube array (19.8 W/m K [19]) and silver particle grease (9.0 W/m K [23]). In spite of the low thermal conductivity, the thermal contact conductance is high due to the low interfacial thermal resistivity.

The thickness of the paste coating is 7–11 μm, which is larger than the value reported by Lin and Chung [11] for thermal pastes (not in a coating form) by 1–2 orders of magnitude (0.4–0.6 μm). There are two reasons for this difference: (i) the flexible graphite core sheet surface is much rougher than the proximate copper surfaces, thus providing larger cavities for the paste to be retained; (ii) the paste in Ref. [11] is tested under uniaxial pressure applied to an effectively infinite surface, so the paste spread freely, resulting in a small thickness. In contrast, in this work, the surface tension of the paste at the edge of the thermal interface area tends to impede the squeezing out of the paste.

4. Conclusion

Comparative evaluation of unmodified flexible graphite, carbon-black-paste-coated flexible graphite and carbon-black-paste-penetrated flexible graphite in their effectiveness as thermal interface materials between copper surfaces of roughness 15 μm and held together at a pressure of 0.46 MPa was conducted. Paste penetration by up to an effective paste thickness of 5 μm increases the thermal contact conductance by up to 350%, 98% and 36% for thicknesses of 50, 130 and 300 μm, respectively. Paste coating up to 10 μm increases the thermal contact conductance by up to 200%, 120% and 65% for thicknesses of 50, 130 and 300 μm, respectively. When the thickness is below 130 μm, the paste-penetrated flexible graphite is superior to the paste-coated flexible graphite, as shown by the thermal contact conductance; at a thickness of 130 μm or above, their performance is similar. Unmodified flexible graphite is much less effective than the paste-coated or paste-penetrated flexible graphite below a thickness of 300 μm. The 2.4 vol.% Cabot paste and the 15 vol.% Tokai paste are similar in their effectiveness. The paste penetration provides relatively low interfacial resistivity and the paste coating provides relatively high through-thickness thermal conductivity. The highest thermal contact conductance achieved is 13.8×10^4 W/m^2 K, as obtained for the 2.4 vol.% Cabot paste-penetrated flexible graphite at a thickness of 26 μm. This value is about 100% higher than thermal greases, phase change materials and carbon nanotube array thermal interface materials. When the 15 vol.% Tokai

paste is used, the flexible graphite cannot be less than 40 μm in thickness.

The thermal conductivity of the paste-penetrated flexible graphite is 3.5–3.9 W/m K and is lower than the value of 5.9 W/m K for the paste-coated or unmodified flexible graphite. This is because the paste penetration under pressure caused partial interruption of the interlocking network of the worms. The thermal conductivity of the paste-penetrated flexible graphite with 1.2 vol.% Cabot paste is lower than that with 2.4 vol.% Cabot paste, due to the lower carbon black content in the former paste.

The interfacial resistivity of the unmodified, paste-coated and paste-penetrated flexible graphite at the interface with copper are 5.4×10^{-5}, $\sim1.3\times10^{-5}$ and $\sim1.4\times10^{-6}$ m^2 K/W, respectively. Both penetration and coating decrease the interfacial resistivity. The high conformability of the coating is the main reason for the low interfacial resistivity for the paste-coated flexible graphite. The boggy layer formed by the penetrated paste is the main reason for the low interfacial resistivity for the paste-penetrated flexible graphite. The paste thickness is 7–11 μm for the coated flexible graphite and effectively 4–5 μm for the corresponding penetrated flexible graphite. The penetration is throughout the thickness.

The thermal contact conductance varies with the thickness, but is insensitive to the fabrication pressure. The pressure of 2000 lb (11.2 MPa) is minimum for maintaining mechanical integrity in the composite.

The carbon black modification (penetration) of flexible graphite increases the thermal contact conductance, thereby enabling the modified flexible graphite to be comparable to or better than any of the previously reported thermal interface materials, which include thermal pastes, paste-coated metal foils, silicone-based thermal pads, carbon nanotube arrays and silver nanofiber arrays.

Appendix A. Supplementary data

Supplementary data associated with this article can be found, in the online version, at doi:10.1016/j.carbon.2010.10.058.

REFERENCES

[1] Chung DDL. Advances in thermal interface materials. Adv Microelectr 2006;33(4):8–11.
[2] Abadi PPSS, Leong CK, Chung DDL. Factors that govern the performance of thermal interface materials. J Electron Mater 2009;38(1):175–92.
[3] Chung DDL. Exfoliation of graphite. J Mater Sci 1987;22(12):4190–8.
[4] Leong CK, Aoyagi Y, Chung DDL. Carbon black pastes as coatings for improving thermal gap-filling materials. Carbon 2006;44(3):435–40.
[5] Luo XC, Chugh R, Biller BC, Hoi YM, Chung DDL. Electronic applications of flexible graphite. J Electron Mater 2002;31(5):535–44.
[6] Luo XC, Chung DDL. Electromagnetic interference shielding reaching 130 db using flexible graphite. Carbon 1996;34(10):1293–4.
[7] Leong CK, Aoyagi Y, Chung DDL. Carbon-black thixotropic thermal pastes for improving thermal contacts. J Electron Mater 2005;34(10):1336–41.
[8] Howe TA, Leong CK, Chung DDL. Comparative evaluation of thermal interface materials for improving the thermal contact between an operating computer microprocessor and its heat sink. J Electron Mater 2006;35(8):1628–35.
[9] Lin C, Chung DDL. Effect of carbon black structure on the effectiveness of carbon black thermal interface pastes. Carbon 2007;45(15):2922–31.
[10] Leong CK, Chung DDL. Carbon black dispersions and carbon–silver combinations as thermal pastes that surpass commercial silver and ceramic pastes in providing high thermal contact conductance. Carbon 2004;42(11):2323–7.
[11] Lin C, Chung DDL. Graphite nanoplatelet pastes vs. carbon black pastes as thermal interface materials. Carbon 2009;47(1):295–305.
[12] Chung DDL. Graphite. J Mater Sci 2002;37(8):1475–89.
[13] Wei X, Liu L, Zhang J, Shi J, Guo Q. Mechanical, electrical, thermal performances and structure characteristics of flexible graphite sheets. J Mater Sci 2010;45(9):2449–55.
[14] Lide DR. CRC handbook of chemistry and physics. 90th ed. Boca Raton: CRC Press; 2009. p. 12–198.
[15] Li J, Sham ML, Kim JK, Marom G. Morphology and properties of UV/ozone treated graphite nanoplatelet/epoxy nanocomposites. Compos Sci Technol 2007;67(2):296–305.
[16] Anderson SH, Chung DDL. Exfoliation of intercalated graphite. Carbon 1984;22(3):253–63.
[17] Sarvar F, Whalley DC, Conway PP. Thermal interface materials – a review of the state of the art. In: The 1st electronics system integration technology conference, vol. 2. Dresden, Germany: IEEE; 2006. p. 1292–302.
[18] Gwinn JP, Webb RL. Performance and testing of thermal interface materials. Microelectr J 2003;34(3):215–22.
[19] Wang H, Feng JY, Hu XJ, Ng KM. Reducing thermal contact resistance using a bilayer aligned CNT thermal interface material. Chem Eng Sci 2010;65(3):1101–8.
[20] Zhang K, Yuan MF, Wang N, Miao JY, Xiao GW, Fan HB. Thermal interface material with aligned CNT and its application in HB-LED packaging. In: Proceedings of the 56th electronic components and technology conference. San Diego, CA: IEEE; 2006. p. 177.
[21] Xu J, Munari A, Dalton E, Mathewson A, Razeeb KM. Silver nanowire array–polymer composite as thermal interface material. J Appl Phys 2009;106(12):124310-1–7.
[22] Liu Z, Chung DDL. Boron nitride particle filled paraffin wax as a phase-change thermal interface material. J Electron Packaging 2006;128(4):319–23.
[23] Maguire L, Behnia M, Morrison G. Systematic evaluation of thermal interface materials – a case study in high power amplifier design. Microelectr Reliab 2005;45(3–4):711–25.
[24] Lin C, Chung DDL. Nanoclay paste as thermal interface material for smooth surfaces. J Electron Mater 2008;37(11):1698–709.
[25] Xu Y, Luo X, Chung DDL. Lithium doped polyethylene-glycol-based thermal interface pastes for high thermal contact conductance. J Electron Packaging 2002;124(3):188–91.